ENERGY ABSORPTION OF ROCK FRAGMENTATION UNDER IMPULSIVE LOADS WITH DIFFERENT WAE FORMS[1]

Li, Xibing Lai, Haihui Gu, Desheng
Central-South University of Technology, Changsha 410083, China

ABSTRACT

In order to investigate the effects of stress waveforms on energy dissipation and the degree of fragmentation of rock, SHPB experiments on rock using rams with different structures and geometries have been performed. The efficiency of energy absorption and post-fragmentation grain sizes under different loading conditions have been determined. The results show that both energy absorption and the degree of fragmentation of rock are related to the shapes of incident stress waves. From the view of energy economization, the approximately symmetric bell-shaped pulse produced by a truncated cone ram is apparently superior to an exponentially-attenuating pulse provided that the incident energy is great enough to fragment the rock. But no matter what the intensities and shapes of the loading pulses are, the maximum energy absorption of rock can not be more than 50 % of the incident energy.

Key words: rock fragmentation dynamics stress wave dissipation and economization of energy

1 INTRODUCTION

Most methods used in rock fragmentation are based on dynamic transient loading. Recently, a number of studies of rock dynamic fracture and fragmentation have been performed under stress wave loading conditions using Split-Hopkinson Pressure Bar (SHPB) and similar devices. Valuable results concerning energy absorption by unconfined cylindrical specimens of rock at room temperature have also been obtained[1-4]. But until now, the research was mainly focused on the effect of the duration and amplitude of stress wave fragmentation, and the incident stress waves were generated by cylindrical rams of the same material and with the same cross-sectional area as the incident bar of a SHPB and the wave shape is approximately rectangular. In fact, in many practical engineering as percussive drilling the shapes of incident stress pulses are often not the same because machines with different impacting pistons generate loading pulses of the different shapes.

In the 1960s, some researchers studied the influence of the shapes of stress waves on the efficiency of energy transfer from drill rods to rock and obtained the most favourable incident stress wave shape corresponding to the maximum efficiency[5-6]. But this efficiency did not clearly indicate the ratio of energy consumed in rock fragmentation to incident energy. Part of the energy transfered to the rock will be dissipated in the form of elastic wave, which are apparently relevant to the shapes of incident stress waves. The purpose of this paper is to investigate the energy absorption and fragmentation degree of rock under impulsive loading with different stress wave shapes. 6

[1]Project sponsored by the National Natural Science Foundation of China under Grant No. 58974150; Manusscript recieved December 24, 1991

rams with different geometries corresponding to different incident stress wave were designed and a series of SHPB tests for 4 typical rocks were carried out.This paper mainly introduces and discusses the effects of the shapes of stress waves on energy absorption and the degree of fragmentation of rock.

2 EXPERIMENTAL

2.1 *Experimental Set-up*

The experimental set-up, in which the one-dimensional stress condition is strictly satisfied, is shown in Fig. 1. The specimen of rock was sandwiched between two cylindrical steel bars, 1,200 mm in length and 22 mm in diameter, forming a SHPB. The density(ρ_e) and the sonic velocity (C_e) of the steel bars were 7.784 $\times 10^3$ kg / m^3 and 5, 606.5 m / s respectively.

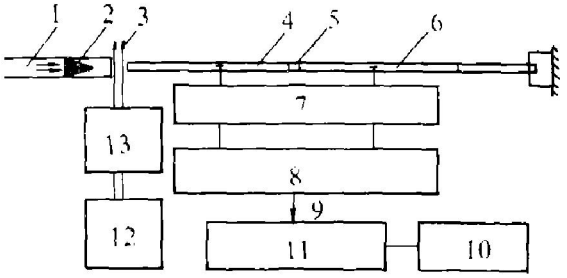

Fig. 1 Experimental set-up

1—compressed air gun; 2—ram; 3—laser; 4—input bar; 5—rock specimen; 6—output bar; 7—superdynamic amplifier; 8—transient recorder; 9—adaptor; 10—printer; 11—computer; 12—timer; 13—transfer and amplifier

The geometrical structure of the rams used in this experiment and the corresponding incident stress pulses are shown in Fig. 2 and 3. From Fig. 3 it can be seen that the durations of the stress waves for rectangular shaped (a), approximately bell-shaped (b), and exponentially attenuating waves (f) were approximately 100 μs. Because the pulse durations primarily depend on the geometrical structure of the impacting rams, they were not changed with terminal ram velocity which was changed in order to generate various stress pulses with different incident ampiltudes or incident energies. At the middle of the input bar a pair of strain gauges were fixed in diametrically opposite positions so that contributions to the outputs from any bending waves were cancelled. Simlarly, a pair of strain gauges were fixed on the other bar at a distance of 600 mm from the specimen. The outputs of the two pairs of strain gauges were amplified and fed to the inputs of a BC—VI transient-recorder. The recording started just before the arrival of the incident stress pulse σ_I at the strain gauges of the input bar. The digitalized stress wave records obtained with the BC—VI transient recorder were analyzed using a Apple—II digital computer . The following quantities were determined:

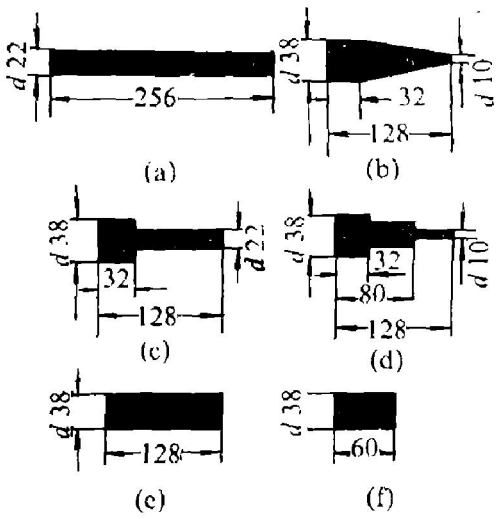

Fig. 2 Geometries of the rams

(1) the energy of the incident stress pulse

$$W_I=(A_eC_e/E_e)\int\sigma_I^2dt \qquad (1)$$

where A_e, C_e and E_e being the cross-sectional area, the sonic velocity, and Young's modolus of the input bar.

(2) the energy of the reflected stress pulse

$$W_R=(A_eC_e/E_e)\int\sigma_R^2dt \qquad (2)$$

(3) the energy of the transmitted stress pulse

$$W_T=(A_eC_e/E_e)\int\sigma_T^2dt \qquad (3)$$

(4) the energy absorbed by the rock specimen

$$W_r = W_I - (W_R + W_T) \quad (4)$$

2.2 *Rock Specimens*

Cylindrical specimens, 21.00 mm in diameter (d_s) and 33.60 mm in length (l_s), were prepared from rock blocks of 500 mm × 500 mm × 500 mm. The two ends of each specimen were ground to a parallel tolerance of less than 0.05 mm. Static compression tests of the specimens were carried out on an INSTRON 1342 machine. The types of rock and their compressive strengths σ_s, Young's moduli (E_s), densities(ρ_s), bar acoustic wave velocities (C_s), and deformation work (W_s) were determined and are given in Table 1.

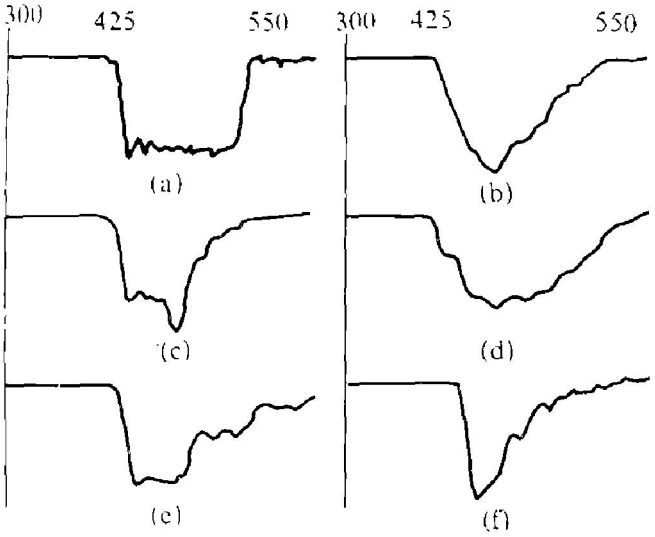

Fig. 3 The forms of incident stress wave corresponding to the rams in Fig. 2

2.3 *The Degree of Fragmention of Rock*

After a specimen was impacted the fragments of the broken rock were collected and sieved using the sieves with mesh diameters of 0.6, 2.5, 6, 9 and 12 mm respectively. The mean grain size of the fragments was calculated as follows

$$d_m = \sum (r_i d_i) / \sum r_i \quad (5)$$

where d_i is the mean grain size of the fragments situated between sieves with successive mesh sizes, and letting the fragments whose sizes are less than 0.6 mm be equal to 0.3 mm, and letting those larger than 12 mm be equal to 13.5 mm; r_i is the wt.−% of the fragments corresponding to d_i.

3 EXPERIMENTAL RESULTS AND DISCUSSION

3.1 *Relation Between Transmitted and Incident Energy*

Fig. 4 shows W_T / W_I vs W_I under the rectangular wave loading condition. Similar results have been obtained for bell-shaped and exponentially attenuating pulse loading. From Fig. 4 it can be seen that W_T not only diminishes with the increase of W_I but also varies with the type of the rock.

3.2 *The Relation Between the Energy Absorbed by Rock* (W_r) *and the Incident Energy* (W_I)

According to the regression results, assuming $W_I = 50$ J, $l / d = 1.6$ and $d = 2.1$ mm, we find that W_T / W_I of sandstone is 35.7 % for the bell-shaped stress-wave, 35.3 % for rectangular stress-wave, and 28.2% for the exponentially attenuating stress-wave. The corresponding figures for granite are 47.7 %, 34.7 %; while those for marble are 43.0 %, 36.1 %, 28.1%.

Table 1 The types and mechanical properties of the rock samples

Types of rock	Degree of homogeneity	ρ 10^3 kg m^{-3}	σ MPa	C km S^{-1}	E GPa	Ω J cm^{-3} Before fracture	After fracture	Total
sandstone	good	2.02	32.43	2.39	15.71	0.0445	0.0345	0.0790
granite	fairly good	2.63	78.58	4.25	39.20	0.1210	0.0925	0.2135
marble	good	2.70	165.9	5.60	79.06	0.2065	0.3365	0.5430
limestone	poor	2.68	110.0	3.79	59.68	0.1375	0.150	0.2935

The above results show that the maximum energy absorption of rock is not more than 50 % of W_r. In fact, according to the experimental results of W_r in all impacts, except the four samples of granite in which the ratio of maximum W_r / W_I is 52.21 %, the maximum energy absorption was generally not more than 50%.

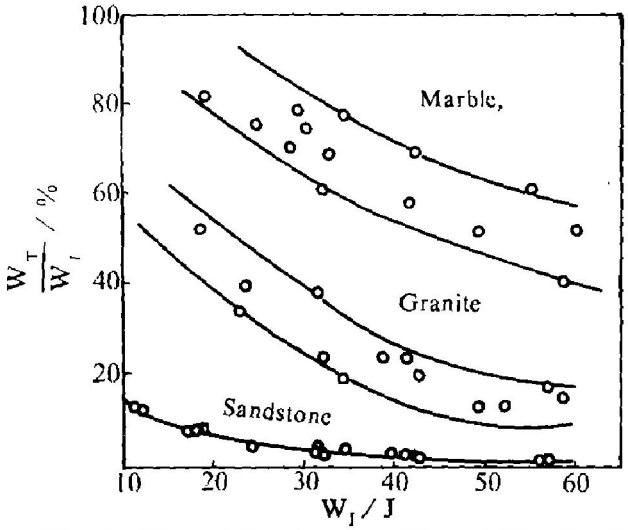

Fig. 4 The relation between W_T and W_I for the rectangular wave loading

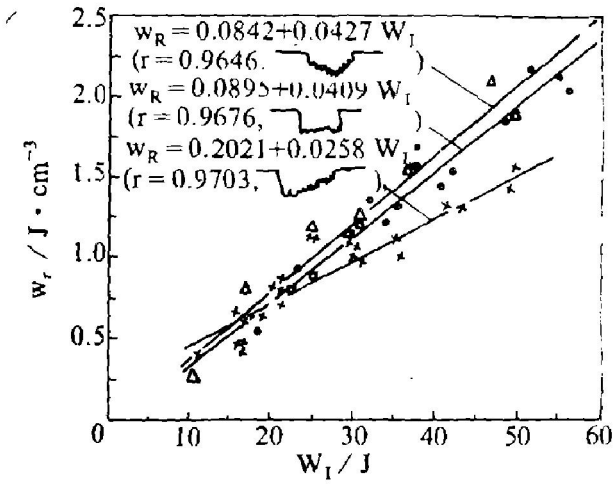

Fig. 5 The relations between energy absorption w_r of granite and incident energy W_I

Fig. 5 illustrate the relation between w_r and W_I of granite loaded by the stress waves shown in Fig. 3 with $W_I = 10 \sim 60$ J. It can be seen that w_r always increases with W_I, but different incident stress waves results in different w_r values. In addition the efficiency of energy absorption of rock for both bell-shaped and rectangular pulses is larger than that for the exponentially attenuating pulse. But for sandstone, because of its serious weathering and lower strength, an incident energy of ~ 20 J can fracture it. So the energy absorption under the exponentially attenuating pulse loading is lower than that of the other pulse loads, and moreover the diversity of the energy absorption of the exponential pulse loading to the other two pulse loading increases with the increasing incident energies. At the range of high loading incident energy the energy absorption of the rectangular pulse approaches that of the bell-shaped pulse, for marble when W_I is larger than its value corresponding to the intersection point of the two curves, the efficiency of energy absorption of rock for the exponential pulse becomes poorer than that for both rectangular and bell-shaped pulses. But when W_I is relatively small an exponential stress wave is superior to both rectangular and bell-shaped stress-waves in energy absorption by the rock.

3. 3 *The Effect of the Loading Waveforms on the Degree of Fragmentation of Rock*

As another example, Fig. 6 shows the grain size distribution of granite fragmented by an approximately bell-shaped stress-wave, it can be seen that the fragmentation degree of rock increases and the grain size composition of the fragments becomes finer and more homogeneous from coarser with the increasing of W_I. The other rock and stress-wave loads yield the similar results to Fig. 6. Fig. 7 presents the relation between mean grain sizes calculated with equation (5) and incident energy W_I and Fig. 8 presents the relation between mean grain sizes and energy absorption per unit volume of granite. From Fig. 6 it can be seen clearly that the post-fragmention grain sizes diminish with increasing W_I. From Fig. 7, one can see that different stress-waves result in different mean grain sizes even if the energy of the incident waves is about the same. But from Fig. 8, it can be seen the stress-wave forms have hardly effect on the degree of rock fragmentation. Thus, those experimental results show that the degree of fragmentation of rock depend mainly on the energy absorption of rock per unit volume, which is mainly used for producing new surface area of rock. When w_r of granite increased to

about 1.5 J.cm^{-3}, the reduction in the grain sizes with increasing w_r is apparently slow, which is perhaps due to a course reasons. First, with the increase of w_r, the kinetic energy transmitted to fragments is increased, and the energy for producing new surface is relatively small. Secondly, high w_r values result in more fine fragments (≤0.6 mm).

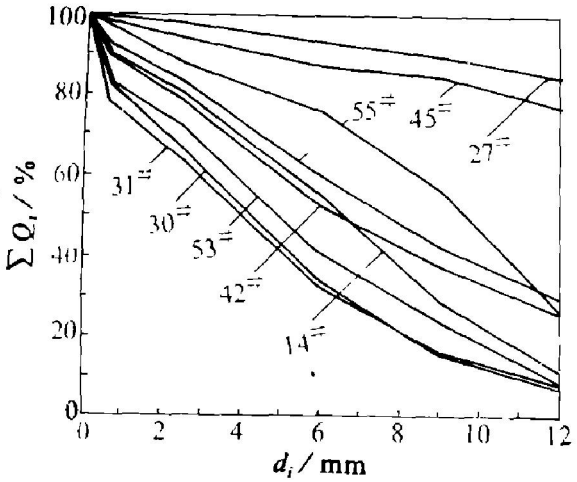

Fig. 6 Granite gain size (d_i) distribrtions under the loading of approximately bell-shaped incident wave

($\sum Q_i$—Cumulative wt. of plus mesh grains)

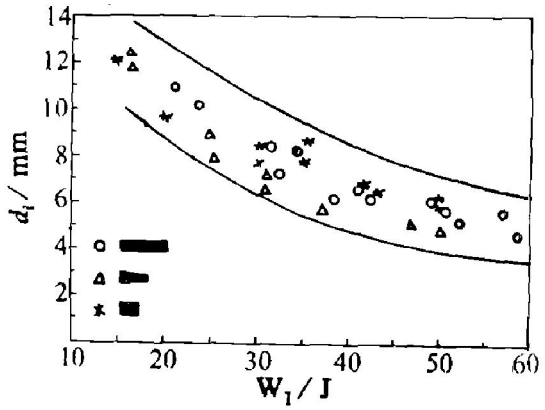

Fig. 7 The relations between the mean grain sizes d_i of granite and incident energy W_1

4 CONCLUSION

(1) The experimental results show that different incident stress-waveforms result in different efficiencies of energy absorption of rock. When the incident energy is great enough for fragmenting rock the efficiency of rock energy absorption for exponentially attenuating stress-wave is less than that for both the approximately bell-shaped and rectangular stress wave;

(2) No matter what the loading pulse waveforms are, the relations between rock energy absorption measured by SHPB and post fragmentation grain sizes can be given in a single linear regression equation, and the dispersion is relatively small. Thus rock energy absorption can indicate the degree of fragmentation rock. While the effects of dynamic fragmentation of rock by different incident waveform loading conditions need to be investigated, this is feasible using SHPB which can measure rock energy absorption and can produce stress pulses with different shapes;

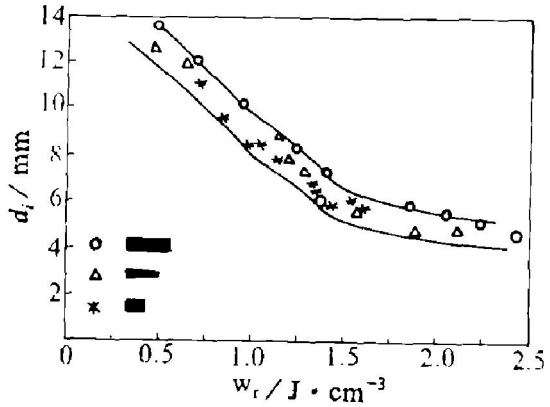

Fig. 8 The relations between mean grain sizes (d_i) and energy absorption w_r of granite

(3) Different stress waveforms result in different degree of fragmentation of rock. This is because energy absorption by rock under different stress waveforms is not the same even if the loading incident energy values are about the same. But no matter what the loading incident waves are the mean grain sizes of the fragments will increase and the grain composition will become finer and more homogeneous with increasing incident energy;

(4) Rock energy absorption increases with increasing incident energy, but the maximun energy absorption of rock hardly surpasses 50 % of incident energy.

(*To be continued on page* № 9)

3.2 *Influence of the Fractal Surface of the Particle on the Size Definition*

The outline of the cross-section and the surface of a rock-fractured particle are fractal. That means the profile perimeter and surface area depend on the step length. Therefore, for a given particle, the perimeter and surface area are not constant. When the smallest self-similar structure on a particle surface can not be known, the definitions of particle size based on two parameters, such as equivalent surface diameter, equivalent volumetricly surface diameter and perimeter diameter are equivocal. Only for a given step length, can the values of a diameter be scaled and compared to each other.

On the basis of the cross-section area and the volume of a particle are constant, volume diameter, projected area diameter, sieve diameter, Feret's diameter, Martin's diameter and unrolled diameter state precisely the meaning of a particle size.

3.3 *The Formula Relating the Length of a Fractal Outline or Area of a Fractal Surface Differ from the Previous One*

When the step length tends toward zero, theoretically, for any particle size, the outline length and surface area should be infinite. However, the particles of rock or ore in nature surely have the smallest self-similar structure so the perimeter P and surface area S can be defined.

Suppose an outline has a fractal dimension D_P, a surface D_S. The volume diameter d_V is chosen as the particle size, according to Ref. [12]. We have

$$P^{1/D_P} \propto V^{1/3} \tag{4}$$

where V is the volume of a particle.

$$S^{1/D_S} \propto V^{1/3} \tag{5}$$

Because $V = kd_V^3$ (k is constant),

$$P \propto d_V^{D_P} = \gamma_1 d_V^{D_P} \tag{6}$$

$$S \propto d_V^{D_P} = \gamma_2 (d_V^{D_S \cdot 2/3})^2 \tag{7}$$

where γ_1 and γ_2 are constants which depend on the smallest self-similar structure of a given particle.

Eqs. 6 and 7 are compared to the traditional equations for perimeter and area in a function of d_V: $P = \gamma_1 d_V^2$, $S = \gamma_2 d_V$. The particle size should be considered as $d_V^{D_P}$ and $d_V^{D_S \cdot 2/3}$.

The surface fractal dimension of rock-fractured particles, which is a characteristic value describing a particle's properties must be measured extensively. This paper serve as the beginning.

REFERENCES

1 Mandelbrot, B. B. Fractal Geometry of Nature. Freeman: San Francisco, 1982: 262.
2 Meloy, T. P., Screening. Washington D.C: AIME, 1969.
3 Meloy, T. P., In: Eng Found Conference. Deerfield, 1971.
4 Meloy, T. P. Powder Technol. 1977, 16(2): 233–254
5 Meloy, T. P., Powder Technol. 1977, 17(1): 27–36.
6 Avnir, D., Farin, D. *et al.* Nature (London). 1984, 308: 261.
7 Pfeifer, P., Avnir, D., J Chem Phy, 1983, 79: 3558.
8 Kaye, B. H., In: Proc Particle Size Analysis Conference, Salford: Chem Soc. Analyt. Div., 1977.
9 Flook, A. G., Powder Technol. 1978, 21: 295–298.
10 Mandlbrot, B. B. Nature, 1984, 308(19):721–722.
11 Clark, N. N. Nature, 1986, 319(20): 625.
12 Takayasu hazijn. (ed) Sheng, Buming (trans.). Fractal Dimension (In Chinese). Beijng: Earthquake Publishing House, 1989.

(*continued from page* № 5)

REFERENCES

1 Hakalehto, K. O., The behaviour of rock under impules loads. Doctor Thesis. Univ of Otaniemi-Helsinki. 1969.
2 Lundberg B., Int J Rock Mech Min Sci & Geomech Abstr. 1976, 13: 187–197.
3 Olsson W. A., Int J Rock Mech Min Sci & Geomech Abstr. 1991, 28: 115–118.
4 Li, Xibing, Lai, Haihui, J Cent-south Inst Min Metall, 1989, 20(6): 595–604
5 Fairhurst, C., Mine Quarry Engng, 1961, 27: 327–328.
6 Lundberg B., Some basic problems in percussive rock destruction. Dissertation. Chalmers Univ of Technology, Gothenburg. 1971.